Article

Cu[Au(CN)](DMSO): Golden Polymorphs That Exhibit Vapochromic Behavior

Julie Lefebvre, Raymond J. Batchelor, and Daniel B. Leznoff

J. Am. Chem. Soc., **2004**, 126 (49), 16117-16125• DOI: 10.1021/ja049069n • Publication Date (Web): 16 November 2004

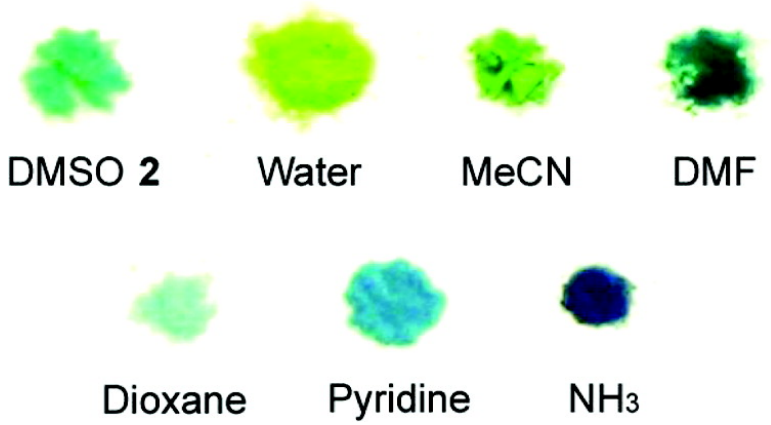

More About This Article

Additional resources and features associated with this article are available within the HTML version:

- Supporting Information
- Links to the 13 articles that cite this article, as of the time of this article download
- Access to high resolution figures
- Links to articles and content related to this article
- Copyright permission to reproduce figures and/or text from this article

View the Full Text HTML

J|A|C|S
ARTICLES
Published on Web 11/16/2004

$Cu[Au(CN)_2]_2(DMSO)_2$: Golden Polymorphs That Exhibit Vapochromic Behavior

Julie Lefebvre, Raymond J. Batchelor, and Daniel B. Leznoff*

Contribution from the Department of Chemistry, Simon Fraser University, 8888 University Drive, Burnaby, B.C., Canada, V5A 1S6

Received February 18, 2004; E-mail: dleznoff@sfu.ca

Abstract: Two polymorphs of an $[Au(CN)_2]$-based coordination polymer, $Cu[Au(CN)_2]_2(DMSO)_2$, one green (**1**) and one blue (**2**), have been identified. In polymorph **1**, alternation of five-coordinate Cu^{II} and $[Au(CN)_2]^-$ units generates 1-D chains, while 2-D corrugated sheets are obtained in polymorph **2**, which contains six-coordinate Cu^{II} centers. Both polymorphs form 3-D networks by virtue of aurophilic interactions of 3.22007(5) Å and 3.419(3) Å, respectively, and show similar weak antiferromagnetic coupling, but have different thermal decomposition temperatures. They both show vapochromic properties and, importantly, despite their significantly different solid-state structures, the vapochromic behavior of the two polymorphs is essentially identical. Upon solvent exchange, both polymorphs convert to the same $Cu[Au(CN)_2]_2(solvent)_x$ complex (solvent = H_2O, CH_3CN, dioxane, *N*,*N*-dimethylformamide, pyridine, NH_3). The $Cu[Au(CN)_2]_2$-(DMF) and $Cu[Au(CN)_2]_2(pyridine)_2$ complexes have very similar 2-D square grid structures, comparable to that of **2**. The solvent molecules adsorbed by $Cu[Au(CN)_2]_2$ bind to the Cu^{II} centers, thereby altering the visible spectrum associated with the Cu^{II} chromophores and the number and frequency of the ν_{CN} as well. The network-stabilizing gold−gold interactions and the flexible coordination sphere of Cu^{II} probably facilitate reversible solvent exchange at room temperature.

Introduction

The controlled design and synthesis of metal-organic coordination polymers from the self-assembly of simple molecular building blocks is of intense interest due to the promise of generating functional materials.[1,2] One common design obstacle in this area is dealing with the facile formation of supramolecular isomers, or polymorphs: the existence of more than one possible type of superstructure for the same building blocks.[3−7] Factors such as the crystallization solvent, temperature, presence of seed crystals, and concentration all play a role in determining which polymorph will be isolated from a given reaction mixture.[5−7] The ability to selectively produce only one polymorph is of vital concern because the materials property targeted usually depends on the three-dimensional solid-state structure. For example, polymorphs of the same material can show different magnetic,[8−10] conducting,[11] luminescent,[12] and zeolitic properties.[13]

Vapochromic materials, which display optical absorption or luminescence changes upon exposure to vapors of volatile organic compounds (VOCs), have been a focus of attention due to their potential applications as chemical sensors.[14−20] For example, when exposed to certain organic solvents, the extended Prussian Blue $Co^{2+}-[Re_6Q_8(CN)_6]^{4-}$ (Q = S, Se) system yields dramatic changes in the visible spectrum that are attributable to the sensed solvent impacting the geometry and hydration around the Co^{II} centers.[20] Several vapochromic compounds based on Au^{I}, Pd^{II}, and Pt^{II} coordination polymers have also been recently reported.[14−19] The vapochromism in these systems is based on changes in both the visible absorption and emission spectra. In the linear $\{Tl[Au(C_6Cl_5)_2]\}_n$ polymer, weak interactions between the Tl atoms and the adsorbed VOC molecules modify slightly the color, and more significantly the emission spectra.[17] On the other hand, changes in the emission spectra

(1) Janiak, C. *J. Chem. Soc., Dalton Trans.* **2003**, 2781−2804.
(2) James, S. L. *Chem. Soc. Rev.* **2003**, *32*, 276−288.
(3) Moulton, B.; Zaworotko, M. J. *Chem. Rev.* **2001**, *101*, 1629−1658.
(4) Batten, S. R.; Murray, K. S. *Aust. J. Chem.* **2001**, *54*, 605−609.
(5) Dunitz, J. D.; Bernstein, J. *Acc. Chem. Res.* **1995**, *28*, 193.
(6) Bernstein, J. *Polymorphism in Molecular Crystals*; Oxford University Press: Oxford, 2002.
(7) Braga, D.; Grepioni, F. *Chem. Soc. Rev.* **2000**, *29*, 229−238.
(8) Leznoff, D. B.; Rancurel, C.; Sutter, J.-P.; Rettig, S. J.; Pink, M.; Paulsen, C.; Kahn, O. *J. Chem. Soc., Dalton Trans.* **1999**, 3593−3599.
(9) Broderick, W. E.; Eichhorn, D. M.; Liu, X.; Toscano, P. M.; Owens, S. M.; Hoffman, B. M. *J. Am. Chem. Soc.* **1995**, *117*, 3641−3642.
(10) Heintz, R. A.; Zhao, H.; Ouyang, X.; Grandinetti, G.; Cowen, J.; Dunbar, K. R. *Inorg. Chem.* **1999**, *38*, 144.
(11) Nakasuji, K.; Sasaki, M.; Kotani, T.; Murata, I.; Enoki, T.; Imaeda, K.; Inokuchi, H.; Kawamoto, A.; Tanaka, J. *J. Am. Chem. Soc.* **1987**, *109*, 6970.
(12) White-Morris, R. L.; Olmstead, M. M.; Balch, A. L. *J. Am. Chem. Soc.* **2003**, *125*, 1033−1040.
(13) Soldatov, D. V.; Ripmeester, J. A. *Chem. Eur. J.* **2001**, *7*, 2979−2994.
(14) White-Morris, R. L.; Olmstead, M. M.; Jiang, F.; Tinti, D. S.; Balch, A. L. *J. Am. Chem. Soc.* **2002**, *124*, 2327−2336.
(15) Mansour, M. A.; Connick, W. B.; Lachicotte, R. J.; Gysling, H. J.; Eisenberg, R. *J. Am. Chem. Soc.* **1998**, *120*, 1329−1330.
(16) Rawashdeh-Omary, M. A.; Omary, M. A.; Fackler, J. P., Jr.; Galassi, R.; Pietroni, B. R.; Burini, A. *J. Am. Chem. Soc.* **2001**, *123*, 9689−9691.
(17) Fernandez Eduardo, J.; Lopez-De-Luzuriaga Jose, M.; Monge, M.; Olmos, M. E.; Perez, J.; Laguna, A.; Mohamed Ahmed, A.; Fackler John, P., Jr. *J. Am. Chem. Soc.* **2003**, *125*, 2022−2023.
(18) Exstrom, C. L.; Sowa, J. R., Jr.; Daws, C. A.; Janzen, D.; Mann, K. R.; Moore, G. A.; Stewart, F. F. *Chem. Mater.* **1995**, *7*, 15−17.
(19) Drew, S. M.; Janzen, D. E.; Buss, C. E.; MacEwan, D. I.; Dublin, K. M.; Mann, K. R. *J. Am. Chem. Soc.* **2001**, *123*, 8414−8415.
(20) Beauvais, L. G.; Shores, M. P.; Long, J. R. *J. Am. Chem. Soc.* **2000**, *122*, 2763−2772.

of $[Pt(CN-R)_4][M(CN)_4]$ (R = *iso*-C_3H_7 or $C_6H_4-C_nH_{2n+1}$; n = 6, 10, 12, 14 and M = Pt, Pd) occur when metal−metal distances are modified due to the presence of VOC molecules in lattice voids; small changes in the absorption spectrum can also be observed.[18,21] Another example is the trinuclear Au^I complex with carbeniate bridging ligands, for which its luminescence is quenched in the solid-state when C_6F_6 vapor is adsorbed due to the disruption of Au−Au interactions.[16]

Some of these vapochromic materials have recently been incorporated in chemical sensor devices. For example, $[Au(PPh_2C(CSSAuC_6F_5)PPh_2Me)_2][ClO_4]$ has been used in the development of an optical fiber volatile organic compound sensor.[22] A vapochromic light emitting diode[23] and a vapochromic photodiode[24] have also been built using tetrakis(*p*-dodecylphenylisocyano)platinum tetranitroplatinate and bis(cyanide)bis(*p*-dodecylphenylisocyanide)platinum(II), respectively.

In this context, we have prepared a new $[Au(CN)_2]$-based coordination polymer and identified two polymorphs, both of which show vapochromic properties. The vapochromism can be readily observed both by visible color changes and also by large IR changes in the ν_{CN} region. Importantly, despite significantly different solid-state structures, the vapochromic behavior of the two polymorphs is essentially identical, indicating that the formation of different polymorphs in this case is not a hindrance to accessing consistent solid-state properties.

Experimental Section

General Procedure and Physical Measurements. All manipulations were performed in air. All the reagents were obtained from commercial sources and used as received. Infrared spectra were recorded as KBr pressed pellets on a Thermo Nicolet Nexus 670 FT-IR spectrometer. Microanalyses (C, H, N) were performed at Simon Fraser University by Mr. Miki Yang. Magnetic susceptibilities were measured on polycrystalline samples at 1 T between 2 and 300 K using a Quantum Design MPMS-5S SQUID magnetometer. All data were corrected for temperature independent paramagnetism (TIP), the diamagnetism of the sample holder, and the constituent atoms (by use of Pascal constants).[25] Solid-state UV−visible reflectance spectra were measured using an Ocean Optics SD2000 spectrophotometer equipped with a tungsten halogen lamp. Thermogravimetric analysis (TGA) data were collected using a Shimadzu TGA-50 instrument in an air atmosphere.

Synthetic Procedures. CAUTION. Although we have experienced no difficulties, perchlorate salts are potentially explosive and should be used in small quantities and handled with care.

Synthesis of $Cu[Au(CN)_2]_2(DMSO)_2$, 1. A 0.5 mL DMSO solution of $Cu(ClO_4)_2\cdot 6H_2O$ (0.037 g, 0.1 mmol) was added to a 0.5 mL DMSO solution of $KAu(CN)_2$ (0.057 g, 0.2 mmol). Green crystals of $Cu[Au(CN)_2]_2(DMSO)_2$ were obtained by slow evaporation over several days, filtered, and air-dried. Yield: 0.050 g, 70%. Anal. Calcd. for $C_8H_{12}N_4Au_2CuO_2S_2$: C, 13.39; H, 1.69; N, 7.81. Found: C, 13.43; H, 1.72; N, 7.61. IR (KBr): 3005(w), 2915(w), 2184(s), 2151(m), 1630(w), 1426(w), 1408(w), 1321(w), 1031(m), 993(s), 967(m), 720(w), 473(m) cm^{-1}. The same product can be obtained by absorption of DMSO by $Cu[Au(CN)_2]_2(H_2O)_2$.

Synthesis of $Cu[Au(CN)_2]_2(DMSO)_2$, 2. A 0.2 mL DMSO solution of $Cu(ClO_4)_2\cdot 6H_2O$ (0.037 g, 0.1 mmol) was added to a 0.4 mL DMSO solution of $KAu(CN)_2$ (0.057 g, 0.2 mmol). Blue needles of $Cu[Au(CN)_2]_2(DMSO)_2$ formed after 1 h and were filtered and dried under N_2. Yield: 0.057 g, 80%. Anal. Calcd. for $C_8H_{12}N_4Au_2CuO_2S_2$: C, 13.39; H, 1.69; N, 7.81. Found: C, 13.50; H, 1.76; N, 7.62. IR (KBr): 3010(w), 2918(w), 2206(m), 2194(s), 2176(m), 2162(m), 1631(w), 1407(w), 1316(w), 1299(w), 1022(m), 991(s), 953(m), 716(w), 458(m) cm^{-1}.

Synthesis of $Cu[Au(CN)_2]_2(DMF)$, 3. A 2 mL DMF solution of $Cu(ClO_4)_2\cdot 6H_2O$ (0.037 g, 0.1 mmol) was prepared. This solution was added to a 3 mL DMF solution of $KAu(CN)_2$ (0.057 g, 0.2 mmol). A dark blue-green mixture of powder and crystals of $Cu[Au(CN)_2]_2(DMF)$ was obtained after several days of slow evaporation and was filtered and air-dried. Yield: 0.033 g, 52%. Anal. Calcd for $C_7H_7N_5Au_2CuO$: C 13.25, H 1.11, N 11.04. Found: C 13.26, H 1.11, N 11.30. IR (KBr): 2927(w), 2871(w), 2199(s), 2171(shoulder), 1665(s), 1660(s), 1492(w), 1434(w), 1414(w), 1384(m), 1251(w), 1105(w), 674(w), 516(w), 408(w) cm^{-1}. Single crystals of **3** were obtained by dissolving $Cu[Au(CN)_2]_2(H_2O)_2$ (**5**) in DMF and allowing the solution to evaporate very slowly. The single crystals and the crystal/powder mixture as prepared above had identical IR spectra. The same product can also be obtained by vapor absorption of DMF by several $Cu[Au(CN)_2]_2(solvent)_x$ complexes.

Synthesis of $Cu[Au(CN)_2]_2(pyridine)_2$, 4. A 10 mL pyridine/water/methanol (5:47.5:47.5) solution of $Cu(ClO_4)_2\cdot 6H_2O$ (0.111 g, 0.3 mmol) was prepared. This solution was added to a 10 mL pyridine/water/methanol (5:47.5:47.5) solution of $KAu(CN)_2$ (0.171 g, 0.59 mmol). A blue powder of $Cu[Au(CN)_2]_2(pyridine)_2$ was obtained immediately and was filtered and air-dried. Yield: 0.163 g, 75%. Anal. Calcd for $C_{14}H_{10}N_6Au_2Cu$: C 23.36, H 1.40, N 11.68. Found: C 23.52, H 1.44, N 11.58. IR (KBr): 3116(w), 3080(w), 2179(s), 2167(s), 2152(s), 2144(m), 1607(m), 1449(m), 1445(s), 1214(m), 1160(w), 1071(m), 1044(w), 1019(m), 758(s), 690(s), 642(m) cm^{-1}. Single crystals of **4** were obtained by slow evaporation of the remaining solution. The crystals and powder had identical IR spectra. The same product can also be obtained by vapor absorption of pyridine by several $Cu[Au(CN)_2]_2(solvent)_x$ complexes.

Synthesis of $Cu[Au(CN)_2]_2(H_2O)_2$, 5. A 10 mL aqueous solution of $Cu(ClO_4)_2\cdot 6H_2O$ (0.259 g, 0.7 mmol) was prepared and added to a 10 mL aqueous solution of $KAu(CN)_2$ (0.403 g, 1.4 mmol). A pale green powder of $Cu[Au(CN)_2]_2(H_2O)_2$ formed immediately and was filtered and air-dried. Yield: 0.380 g, 91%. The same product can be obtained by vapor absorption of water by several $Cu[Au(CN)_2]_2(solvent)_x$ complexes. Anal. Calcd for $C_4H_4N_4Au_2CuO_2$: C 8.04, H 0.67, N 9.38. Found: C 8.18, H 0.71, N 9.22. IR (KBr): 3246(m), 2217(s), 2194(vw), 2171(s), 1633(w) cm^{-1}.

Synthesis of $Cu[Au(CN)_2]_2$, 6. $Cu[Au(CN)_2]_2(H_2O)_2$ was heated (150 °C) in vacuo to yield green-brown $Cu[Au(CN)_2]_2$. The yield is quantitative, with no ν_{CN} peaks for hydrated **5** observable. Anal. Calcd. for $C_4N_4Au_2Cu$: C 8.56, H 0, N 9.98. Found: C 8.68, H trace, N 9.80. IR (KBr): 2191(s), 1613(vw), 530(m) cm^{-1}.

Synthesis of $Cu[Au(CN)_2]_2(CH_3CN)_2$, 7. A 1 mL CH_3CN solution of $Cu(ClO_4)_2\cdot 6H_2O$ (0.037 g, 0.1 mmol) was prepared and added to a 2 mL CH_3CN solution of $KAu(CN)_2$ (0.057 g, 0.2 mmol). A green powder of $Cu[Au(CN)_2]_2(CH_3CN)_2$ precipitated immediately along with a white powder of $KClO_4$. To prevent the replacement of CH_3CN by atmospheric water, the solvent was removed under vacuum and the $KClO_4$ side product was not removed through washing and filtering. Anal. Calcd for $Cu[Au(CN)_2]_2(CH_3CN)_2 + 2(KClO_4)$ ($C_8H_6N_6Au_2Cl_2CuK_2O_8$): C 10.44, H 0.65, N 9.12. Found: C 10.99, H 0.57, N 8.69. IR (KBr): 2297(w), 2269(w), 2192(s), 1600(w), 1445(w), 1369(w), 1088(s), 941(w), 925(w), 752(w), 695(w), 626(m), 512(w), 468(w), 419(w) cm^{-1}. The same product (without $KClO_4$) can be obtained by vapor absorption of acetonitrile by $Cu[Au(CN)_2]_2(DMSO)_2$ (**1** or **2**).

Synthesis of $Cu[Au(CN)_2]_2(dioxane)(H_2O)$, 8. A 2 mL dioxane/water (2:1) solution of $Cu(ClO_4)_2\cdot 6H_2O$ (0.037 g, 0.1 mmol) was prepared. This solution was added to a 4 mL dioxane/water (2:1)

(21) Buss, C. E.; Anderson, C. E.; Pomije, M. K.; Lutz, C. M.; Britton, D.; Mann, K. R. *J. Am. Chem. Soc.* **1998**, *120*, 7783−7790.
(22) Bariain, C.; Matias, I. R.; Romeo, I.; Garrido, J.; Laguna, M. *Appl. Phys. Lett.* **2000**, *77*, 2274−2276.
(23) Kunugi, Y.; Mann, K. R.; Miller, L. L.; Exstrom, C. L. *J. Am. Chem. Soc.* **1998**, *120*, 589−590.
(24) Kunugi, Y.; Miller, L. L.; Mann, K. R.; Pomije, M. K. *Chem. Mater.* **1998**, *10*, 1487−1489.
(25) Kahn, O. *Molecular Magnetism*; VCH: Weinheim, 1993.

Table 1. Crystallographic Data and Structural Refinement Details

	1 (green)	**2** (blue)	**3**	**4**
empirical formula	$C_8H_{12}N_4Au_2CuO_2S_2$	$C_8H_{12}N_4Au_2CuO_2S_2$	$C_7H_7N_5Au_2CuO$	$C_{14}H_{10}N_6Au_2Cu$
fw	717.82	717.82	634.65	719.76
crystal system	monoclinic	triclinic	monoclinic	monoclinic
space group	*C*2/*c*	P$\bar{1}$	*C*2/*c*	$P2_1/c$
a, Å	11.5449(15)	7.874(7)	12.8412(10)	7.3438(7)
b, Å	14.191(4)	12.761(11)	14.5056(8)	14.1201(10)
c, Å	11.5895(12)	16.207(13)	13.9932(9)	8.2696(6)
α, deg	90	89.61(7)	90	90
β, deg	112.536(9)	82.29(7)	96.064(3)	94.082(3)
γ, deg	90	88.57(7)	90	90
V, Å^3	1753.8(6)	1613.2(24)	2591.9(3)	855.34(12)
Z	4	2	8	4
T, K	293	293	293	293
λ, Å	0.70930	1.54180	1.54180	1.54180
ρ_{calcd}, g·cm^{-3}	2.719	2.955	3.253	2.794
μ, mm^{-1}	18.079	37.500	43.542	33.103
$R_1{}^a(I > x\sigma(I))^b$	0.042	0.062	0.032	0.028
$wR_2{}^a(I > x\sigma(I))^b$	0.047	0.082	0.046	0.040
goodness of fit	2.20	1.38	0.93	1.00

[a] Function minimized $\Sigma w(|F_o| - |F_c|)^2$ where $w^{-1} = \sigma^2(F_o) + 0.0001F_o^2$, $R = \Sigma||F_o| - |F_c||/\Sigma|F_o|$, $R_w = [\Sigma w(|F_o| - |F_c|)^2 / \Sigma w|F_o|^2)]^{1/2}$. [b] For **1**, $x = 2.5$; for **2**, **3**, and **4**, $x = 3$.

solution of $KAu(CN)_2$ (0.057 g, 0.2 mmol). A pale blue-green powder of $Cu[Au(CN)_2]_2$(dioxane)(H_2O) was obtained immediately and was filtered and air-dried. Yield: 0.057 g, 85%. The same product can be obtained by vapor absorption of dioxane by several $Cu[Au(CN)_2]_2$-(solvent)$_x$ complexes (the water molecule included in this case is from ambient moisture). Anal. Calcd for $C_8H_{10}N_4Au_2CuO_3$: C 14.39, H 1.51, N 8.39. Found: C 14.31, H 1.21, N 8.43. IR (KBr): 2976(m), 2917(m), 2890(w), 2862(m), 2752(w), 2695(w), 2201(s), 2172(w), 1451(m), 1367(m), 1293(w), 1255(s), 1115(s), 1081(s), 1043(m), 949(w), 892(m), 871(s), 705(w), 610(m), 515(m), 428(m) cm^{-1}.

Synthesis of $Cu[Au(CN)_2]_2(NH_3)_4$, 9. This product was obtained by vapor absorption of NH_3 by several $Cu[Au(CN)_2]_2$(solvent)$_x$ complexes. The yield is quantitative as shown by IR. Anal. Calcd. for $C_4H_{12}N_8Au_2Cu$: C 7.63, H 1.92, N 17.80. Found: C 7.56, H 1.98, N 17.71. IR (KBr): 3359(s), 3328(s), 3271(s), 3212(m), 3182(m), 2175(m), 2148(s), 1639(m), 1606(m), 1243(s), 685(s), 435(w) cm^{-1}.

X-ray Crystallographic Analysis. $Cu[Au(CN)_2]_2(DMSO)_2$ 1 and 2, $Cu[Au(CN)_2]_2$(DMF) 3 and $Cu[Au(CN)_2]_2$(pyridine)$_2$ 4. Crystallographic data for all structures are collected in Table 1. Crystals **1**, **3**, and **4** were mounted on glass fibers using epoxy adhesive and crystal **2** was sealed in a glass capillary. Crystal **1** was a green rectangular plate (0.09 × 0.12 × 0.3 mm^3), crystal **2** was a pale blue needle (0.11 × 0.11 × 0.2 mm^3), crystal **3** was a green needle (0.09 × 0.09 × 0.15 mm^3) and crystal **4** was a dark blue platelet (0.02 × 0.06 × 0.15 mm^3).

For **1**, data in the range $4° < 2\theta < 55°$ were recorded using the diffractometer control program DIFRAC[26] and an Enraf Nonius CAD4F diffractometer. The NRCVAX Crystal Structure System was used to perform psi-scan absorption correction (transmission range: 0.0301−0.1726) and data reduction, including Lorentz and polarization corrections.[27] All non-hydrogen atoms were refined anisotropically. Full matrix least-squares refinement (1231 reflections included) on *F* (93 parameters) converged to $R_1 = 0.042$, $wR_2 = 0.047$ ($I_o > 2.5\sigma(I_o)$).

For **2**, **3**, and **4**, data in the ranges $6.9° < 2\theta < 136.1°$, $9.2° < 2\theta < 144.0°$ and $12.0° < 2\theta < 142.6°$, respectively, were recorded on a Rigaku RAXIS RAPID imaging plate area detector. A numerical absorption correction was applied (transmission range: 0.019−0.161, 0.0070−0.0199, and 0.3484−0.5826) and the data were corrected for Lorentz and polarization effects.[28] For **2**, the Au, Cu and S atoms were refined anisotropically, whereas the remainder were refined isotropically. For **3** and **4**, all non-hydrogen atoms were refined anisotropically. Full matrix least-squares refinement on *F* was performed on **2**, **3** and **4**, the data converging to the following results: for **2**, $R_1 = 0.062$, $wR_2 = 0.082$ ($I_o > 3.0\sigma(I_o)$, 2026 reflections included, 205 parameters); for **3**, $R_1 = 0.0315$, $wR_2 = 0.0456$ ($I_o > 3.0\sigma(I_o)$, 1538 reflections included, 148 parameters); for **4**, $R_1 = 0.0276$, $wR_2 = 0.0401$ ($I_o > 3.0\sigma(I_o)$, 1021 reflections included, 107 parameters).

All structures were refined using CRYSTALS.[29] The structures were solved using Sir 92 and expanded using Fourier techniques. Hydrogen atoms were included geometrically in all structures but not refined. Diagrams were made using Ortep-3 (version 1.076)[30] and POV−Ray (version 3.6.0).[31] Selected bond lengths and angles for **1**−**4** are reported in Tables 2 to 5, respectively.

Results

Synthesis. The reaction of Cu^{II} salts with $KAu(CN)_2$ in dimethyl sulfoxide (DMSO) produced two different compounds, depending on the total concentration of starting reagents. In dilute solution, green crystals of polymorph **1** formed slowly, whereas blue crystals of polymorph **2** were obtained rapidly in a highly concentrated solution. The IR spectra of **1** and **2** show different features (Table 6); the higher-energy bands likely correspond to bridging CN-groups, whereas the lower-energy bands are due to either free or loosely bound CN-groups.[32] The X-ray crystal structures of **1** and **2** revealed two different polymeric networks, both with the same empirical formula $Cu[Au(CN)_2]_2(DMSO)_2$, as confirmed by elemental analysis.

Crystal Structure of the Green $Cu[Au(CN)_2]_2(DMSO)_2$ Polymorph, 1. The five-coordinate Cu^{II} center in **1** has a *τ*-value[33] of 0.44, where $\tau = 0$ is pure square pyramidal and $\tau = 1$ is pure trigonal bipyramidal, suggesting that the coordination geometry could be considered equally distorted from either polyhedron. The Cu^{II} center is bound to two

(26) Gabe, E. J.; White, P. S.; Enright, G. D. *DIFRAC A Fortran 77 Control Routine for 4-Circle Diffractometers*; N. R. C.: Ottawa, 1995.
(27) Gabe, E. J.; LePage, Y.; Charland, J.-P.; Lee, F. L.; White, P. S. *J. Appl. Crystallogr.* **1989**, *22*, 384.
(28) Higashi, T. *Program for Absorption Correction*; Rigaku Corporation: Tokyo, Japan, 1999.
(29) Watkin, D. J.; Prout, C. K.; Carruthers, J. R.; Betteridge, P. W.; Cooper, R. I. *CRYSTALS Issue 11* Chemical Crystallography Laboratory, University of Oxford, Oxford, England, 1999.
(30) Farrugia, L. J. *J. Appl. Crystallogr.* **1997**, *30*, 565.
(31) Fenn, T. D.; Ringe, D.; Petsko, *J. Appl. Crystallogr.* **2003**, *36*, 944−947. (Persistence of Vision Raytracing: http://www.povray.org).
(32) Dunbar, K. R.; Heintz, R. A. *Prog. Inorg. Chem.* **1997**, *45*, 283−391.
(33) Addison, A. W.; Rao, T. N.; Reedijk, J.; Van Rijn, J.; Verschoor, G. C. *J. Chem. Soc., Dalton Trans.* **1984**, 1349−1356.

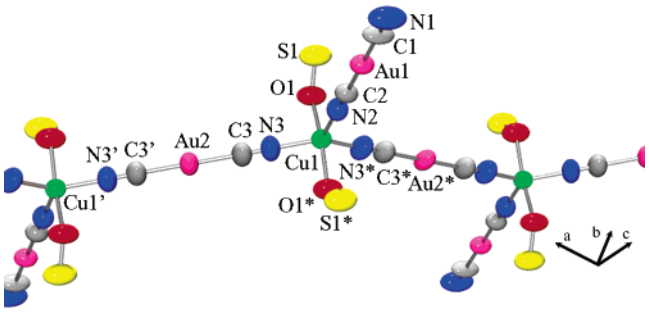

Figure 1. Extended 1-D zigzag chain structure of $Cu[Au(CN)_2]_2(DMSO)_2$ (**1**). DMSO-methyl groups were removed for clarity.

Table 2. Selected Bond Lengths (Å) and Angles (deg) for $Cu[Au(CN)_2]_2(DMSO)_2$ (**1**)[a]

Au(1)−Au(2)	3.22007(5)	Cu(1)−N(2)	2.107(18)
Cu(1)−O(1)	1.949(7)	Cu(1)−N(3)	1.965(11)
O(1)−Cu(1)−O(1*)	167.0(6)	Cu(1)−N(2)−C(2)	180
O(1)−Cu(1)−N(2)	96.5(3)	Cu(1)−N(3)−C(3)	178.6(12)
O(1)−Cu(1)−N(3)	87.3(4)	Au(2)−Au(1)−Au(2)	171.73(3)
O(1*)−Cu(1)−N(3)	88.4(4)	Au(1)−N(1)−C(1)	180
N(2)−Cu(1)−N(3)	109.5(4)	Au(1)−N(2)−C(2)	180
N(3)−Cu(1)−N(3*)	140.9(8)	Au(2)−N(3)−C(3)	178.9(12)
Cu(1)−O(1)−S(1)	127.2(6)	C(1)−Au(1)−C(2)	180

[a] Symmetry transformations: (*) $-x+1, y, -z+1/2$; (′) $-x+1/2, -y-5/2, z+1$.

DMSO−O atoms (O−Cu−O = 167.06°) and three N(cyano) atoms (Figure 1). Selected bond lengths and angles for **1** are listed in Table 2. The asymmetric unit contains two different $[Au(CN)_2]^-$ units: a Cu^{II}-bridging moiety that generates a 1-D chain, and a Cu^{II}-bound dangling group. The chains stack on top of each other parallel to the (101)-plane, forming stacks of chains that are offset to allow interdigitation of the dangling $[Au(CN)_2]^-$ units. Each chain is connected to the four neighboring chains through Au−Au interactions of 3.22007(5) Å between the Au(1) atoms of each dangling group and the Au(2) atoms of the chain backbone (Figure 2 top). The DMSO molecules occupy the channels between the chains; these channels are delineated by both $[Au(CN)_2]$ groups and Au−Au bonds (Figure 2 bottom). A viable Au−Au interaction is considered to exist when the distance between the two atoms is less than 3.6 Å, the sum of the van der Waals radii for gold.[34]

Crystal Structure of the Blue $Cu[Au(CN)_2]_2(DMSO)_2$ Polymorph, 2. The structure of polymorph **2** contains Cu^{II} centers in a Jahn−Teller distorted octahedral geometry, with the two DMSO molecules bound in a *cis*-equatorial fashion (O−Cu−O = 95.2°) rather than in the nearly 180°-arrangement in **1**. Selected bond lengths and angles for **2** are found in Table 3. The four remaining sites (two axial and two equatorial) are occupied by N(cyano) atoms of bridging $[Au(CN)_2]^-$ units, generating corrugated 2-D sheets (Figure 3 top). These 2-D layers stack (Figure 3 bottom) and are held together by weak Au(1)−Au(2) interactions of 3.419(3) Å and perhaps weak Au(3)···Au(4) contacts of 3.592(4) Å. Thus, the color difference between the two polymorphs can be attributed to the different coordination number and geometry around the Cu^{II} centers. That said, the coarse features of **1**, namely the rectangular "channels" filled with DMSO molecules, are also clearly delineated in **2**.

Magnetic Properties. As polymorphs **1** and **2** clearly have significantly different solid-state structures, it follows that their

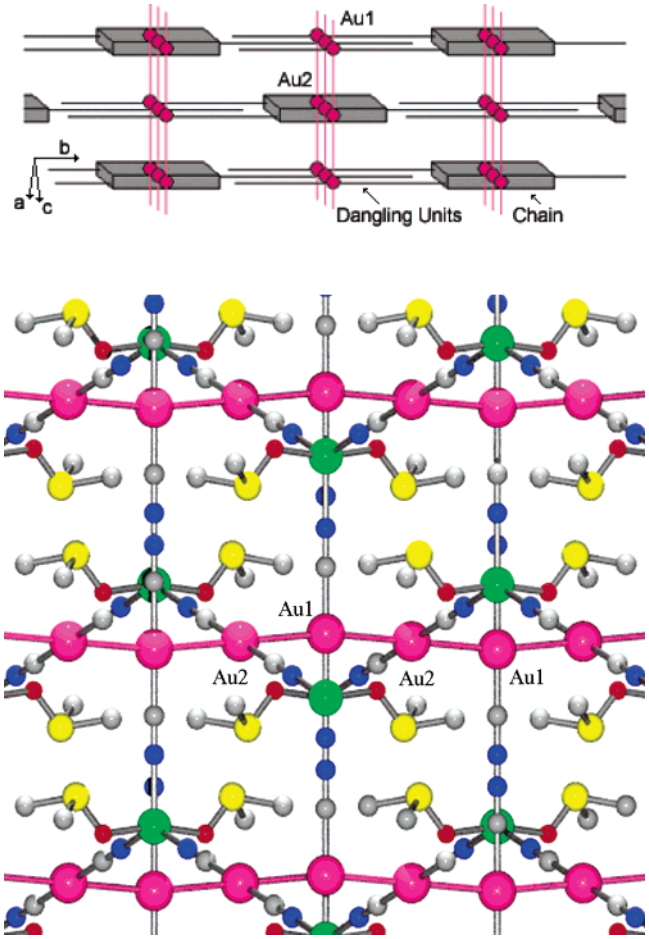

Figure 2. Top: Offset stacks of chains in **1**, viewed down the (101)-plane (slightly tilted). Au−Au bonds connect bridging and dangling $[Au(CN)_2]^-$ units of neighboring chains (pink lines). Bottom: 3-D structure of **1** formed via Au−Au bonding, viewed down the *a*-axis. Color scheme: Au, pink; Cu, green; S, yellow; O, red; N, blue; C, gray.

physical and chemical properties may also vary; this is the case for their solid-state optical reflectance spectra, which show λ_{max} of 550 ± 7 and 535 ± 15 nm respectively (Table 6). To explore this key issue, a series of representative properties were investigated. For example, the magnetic susceptibilities of **1** and **2** were measured at temperatures varying from 300 to 2 K. At 300 K, the effective magnetic moments (μ_{eff}) are 1.98 and 1.93 μ_B for **1** and **2**, respectively, typical for Cu^{II} centers.[35] As the temperature drops, μ_{eff} decreases and reaches 1.74 and 1.67 μ_B at 2 K for **1** and **2** respectively. There is no maximum in either χ_M vs *T* plot. This behavior is consistent with weak antiferromagnetic coupling, probably mediated by the diamagnetic Au^I center.[36−39] Thus, the two polymorphs have similar magnetic properties.

Thermal Stability. Examining the thermal stabilities of **1** and **2** by thermogravimetric analysis (Figure 4), **1** loses its first DMSO molecule from 150 to 190 °C and the other one from

(34) Schmidbaur, H. *Chem. Soc. Rev.* **1995**, *24*, 391.

(35) Carlin, R. L. *Magnetochemistry*; Springer-Verlag: Berlin, Heidelberg, Germany, 1986.
(36) Leznoff, D. B.; Xue, B.-Y.; Patrick, B. O.; Sanchez, V.; Thompson, R. C. *Chem. Commun.* **2001**, 259−260.
(37) Leznoff, D. B.; Xue, B. Y.; Stevens, C. L.; Storr, A.; Thompson, R. C.; Patrick, B. O. *Polyhedron* **2001**, *20*, 1247−1254.
(38) Leznoff, D. B.; Xue, B.-Y.; Batchelor, R. J.; Einstein, F. W. B.; Patrick, B. O. *Inorg. Chem.* **2001**, *40*, 6026−6034.
(39) Colacio, E.; Lloret, F.; Kivekaes, R.; Suarez-Varela, J.; Sundberg, M. R.; Uggla, R. *Inorg. Chem.* **2003**, *42*, 560−565.

Table 3. Selected Bond Lengths (Å) and Angles (deg) for $Cu[Au(CN)_2]_2(DMSO)_2$ (**2**)[a]

Au(1)−Au(2)	3.419(3)	Au(3)···Au(4)	3.592(4)
Cu(1)−O(1)	2.02(3)	Cu(2)−O(3)	1.97(3)
Cu(1)−O(2)	1.95(3)	Cu(2)−O(4)	2.29(3)
Cu(1)−N(11)	2.42(4)	Cu(2)−N(12)	2.11(4)
Cu(1)−N(21)	1.97(4)	Cu(2)−N(22)	2.37(5)
Cu(1)−N(31)	2.42(4)	Cu(2)−N(32)	2.03(5)
Cu(1)−N(41)	1.99(4)	Cu(2)−N(42)	2.00(5)
O(1)−Cu(1)−O(2)	95.2(12)	O(3)−Cu(2)−O(4)	93.0(12)
O(1)−Cu(1)−N(11)	85.9(12)	O(3)−Cu(2)−N(12)	87.8(15)
O(2)−Cu(1)−N(11)	86.4(12)	O(4)−Cu(2)−N(12)	87.0(14)
N(11)−Cu(2)−N(21)	92.7(14)	N(12)−Cu(2)−N(22)	92.3(16)
N(11)−Cu(2)−N(31)	172.7(13)	N(12)−Cu(2)−N(32)	172.0(17)
N(11)−Cu(2)−N(41)	92.6(14)	N(12)−Cu(2)−N(42)	95.2(17)
N(21)−Cu(2)−N(31)	92.6(15)	N(22)−Cu(2)−N(32)	91.4(17)
N(21)−Cu(2)−N(41)	90.7(15)	N(22)−Cu(2)−N(42)	91.2(17)
N(31)−Cu(2)−N(41)	92.3(14)	N(32)−Cu(2)−N(42)	91.8(18)
Cu(1)−O(1)−S(1)	124.9(17)	Cu(2)−O(3)−S(3)	125.4(20)
Cu(1)−O(2)−S(2)	124.4(19)	Cu(2)−O(4)−S(4)	127.9(18)
Cu(1)−N(11)−C(11)	169.2(45)	Cu(2)−N(12)−C(12)	163.5(50)
Cu(1)−N(21)−C(21)	163.5(41)	Cu(2)−N(22)−C(22)	159.5(46)
Cu(1)−N(31)−C(31)	161.7(43)	Cu(2)−N(32)−C(32′)	174.6(45)
Cu(1)−N(41)−C(41)	166.4(33)	Cu(2)−N(42)−C(42)	170.0(45)
C(11)−Au(1)−C(12)	172.7(25)	C(31)−Au(3)−C(32)	172.6(18)
C(21)−Au(2)−C(22*)	175.9(23)	C(41*[b])−Au(4)−C(42)	177.9(20)
Au(1)−C(11)−N(11)	175.8(50)	Au(3)−C(31)−N(31)	171.0(39)
Au(1)−C(12)−N(12)	175.3(58)	Au(3)−C(32)−N(32′[b])	175.6(49)
Au(2)−C(21)−N(21)	173.2(42)	Au(4*[b])−C(41)−N(41)	174.2(38)
Au(2*)−C(22)−N(22)	175.2(56)	Au(4)−C(42)−N(42)	170.1(46)

[a] Symmetry transformations: (*) $-x+1, -y+1, -z+1$; (*[b]) $-x+1, -y, -z+1$; (′) $x+2, y, z-1$; (′[b]) $x-2, y, z+1$.

210 to 250 °C. For polymorph **2** (which has 4 crystallographically distinct DMSO molecules), the first two DMSO molecules are lost between 100 and 135 °C and then 150−190 °C, whereas the two remaining DMSO molecules dissociate around 210−250 °C, comparable with **1**. Both polymorphs are then stable until ∼310 °C, at which point cyanogen (C_2N_2) is released, consistent with the decomposition of the $Cu[Au(CN)_2]_2$ framework.[40] Hence, the thermal stabilities of the two polymorphs with respect to the loss of the first DMSO molecules are significantly different. Differential scanning calorimetry shows no evidence for the thermal interconversion in the solid state from **2** to **1** below the decomposition temperature of **2**.

Vapochromic Behavior. Interestingly, even though both polymorphs are thermally stable up to at least 100 °C, the DMSO molecules can easily be replaced by ambient water vapor at room temperature to yield $Cu[Au(CN)_2]_2(H_2O)_2$ (**5**), as shown by elemental and thermogravimetric analysis. Despite the fact that both polymorphs have different solid-state structures, IR spectroscopy and powder X-ray diffraction show that both polymorphs convert to the same $Cu[Au(CN)_2]_2(H_2O)_2$ (**5**) complex (Table 6). This conversion is reversible, but with a twist: if DMSO vapor is added back to **5**, only the green polymorph $Cu[Au(CN)_2]_2(DMSO)_2$ (**1**) is formed, even if the original DMSO-complex to which H_2O was added was the blue polymorph (**2**). The exchange of DMSO for H_2O can be observed visually from the associated color change (Figure 5).

$Cu[Au(CN)_2]_2(DMSO)_2$ (either **1** or **2**) also displays vapochromic behavior when exposed to a variety of other donor solvent vapors in addition to H_2O. Each $Cu[Au(CN)_2]_2(solvent)_x$ complex can be distinguished easily by its color (Figure 5 and Table 6). In addition, the ν_{CN} region of the IR spectrum for each solvent complex is a characteristic, sensitive signature for that solvent (Table 6). Importantly, this solvent exchange is completely reversible, thus permitting dynamic solvent sensing.

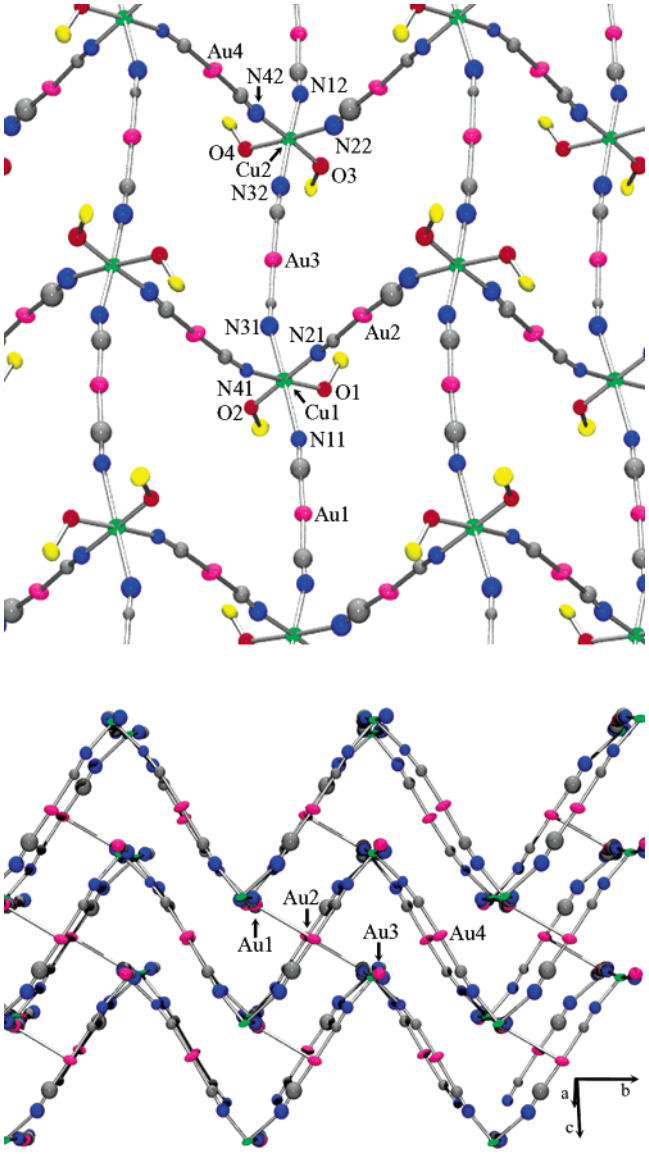

Figure 3. Top: Extended structure of **2** showing the 2-D corrugated layers, viewed down the *a*-axis. DMSO-methyl groups were removed for clarity. Bottom: Layers stacked via aurophilic interactions to yield a 3-D network.

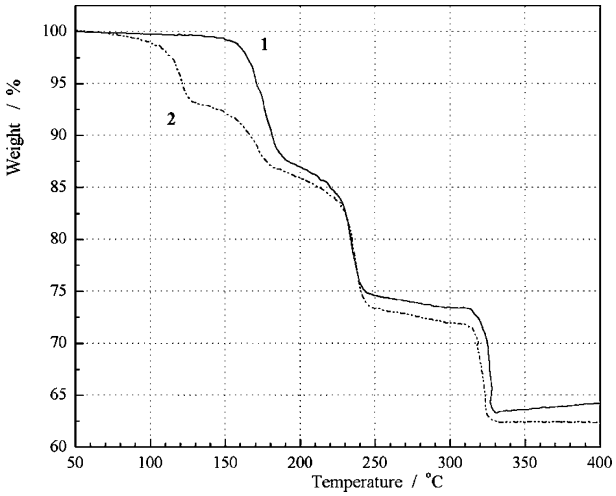

Figure 4. Thermal decomposition of polymorphs **1** and **2**.

(40) Chomic, J.; Cernak, J. *Thermochim. Acta* **1985**, *93*, 93.

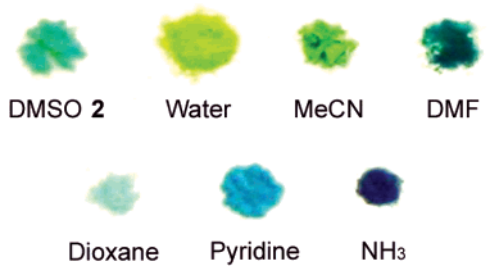

Figure 5. Powder sample of **2** exposed to various solvent vapors.

Table 4. Selected Bond Lengths (Å) and Angles (deg) for $Cu[Au(CN)_2]_2(DMF)$ (**3**)[a]

Au(1)−Au(1*[a])	3.3050(12)	Cu(1)−N(2)	1.990(11)
Au(2)−Au(2*[b])	3.1335(13)	Cu(1)−N(3)	1.961(10)
Cu(1)−O(1)	2.202(12)	Cu(1)−N(4′[b])	1.982(10)
Cu(1)−N(1′)	1.958(10)	O(1)−C(5)	1.202(17)
N(1′[a])-Cu(1)−N(2)	89.8(4)	C(1)−Au(1)−C(2)	176.0(6)
N(1′[a])−Cu(1)−N(3)	88.7(5)	C(3)−Au(2)−C(4)	175.4(6)
N(4′[b])−Cu(1)−N(2)	89.6(5)	Cu(1′[c])−N(1)−C(1)	170.1(12)
N(4′[b])−Cu(1)−N(3)	89.3(5)	Cu(1)−N(2)−C(2)	172.7(14)
N(1′[a])−Cu(1)−N(4′[b])	166.7(5)	Cu(1)−N(3)−C(3)	170.8(12)
N(2)−Cu(1)−N(3)	169.2(5)	Cu(1′[d])−N(4)−C(4)	172.1(12)
O(1)−Cu(1)−N(1′[a])	95.1(5)	Au(1)−C(1)−N(1)	174.9(13)
O(1)−Cu(1)−N(2)	98.3(5)	Au(1)−C(2)−N(2)	177.8(14)
O(1)−Cu(1)−N(3)	92.4(5)	Au(2)−C(3)−N(3)	174.3(13)
O(1)−Cu(1)−N(4′[b])	98.1(5)	Au(2)−C(4)−N(4)	177.5(16)
Cu(1)−O(1)−C(5)	125.4(13)		

[a] Symmetry transformations: (*[a]) $-x-1, y, -z+3/2$; (*[b]) $-x-1, y, -z+1/2$; (′[a]) $x, -y, z-1/2$; (′[b]) $x, -y-1, z+1/2$; (′[c]) $x, -y, z+1/2$; (′[d]) $x, -y-1, z-1/2$.

Hence, starting with a solid of any $Cu[Au(CN)_2]_2(solvent)_x$, addition of a different solvent vapor generates the new complex. The only exceptions occur with very strong donor solvents such as pyridine or ammonia, which bind strongly to the Cu^{II} center and are not easily displaced by other solvents.

Each $Cu[Au(CN)_2]_2(solvent)_x$ complex was also synthesized by reacting Cu^{II} salts with $[Au(CN)_2]^-$ in the appropriate solvent and each was found, by elemental analysis, IR spectroscopy, TGA, and crystallography, to be identical to the complex generated by solvent exchange (Table 6). In every case, elemental analysis and TGA (Table S1) indicate that the number of solvent molecules incorporated into the complex per transition metal center is always the same as the number incorporated by vapor adsorption. This is easily rationalized by the fact that all adsorbed solvent molecules are *ligated* to the Cu^{II} center in a 1:1, 1:2 or, in the case of ammonia, a 1:4 ratio, with no additional loosely trapped solvent molecules in channels (as shown by TGA, Table S1), as is often observed in other porous systems that include solvent.[41−44]

Crystal Structure of $Cu[Au(CN)_2]_2(DMF)$, 3. To better understand the structural changes that occur during a vapochromic response of the DMSO polymorphs, the structures of $Cu[Au(CN)_2]_2(DMF)$ (**3**) and $Cu[Au(CN)_2]_2(pyridine)_2$ (**4**) were investigated. The structure of **3** contains Cu^{II} centers with a square-pyramidal geometry, where the four basal sites are occupied by N(cyano) atoms of bridging $[Au(CN)_2]^-$ units, and the apical site is occupied by an O-bound DMF molecule.

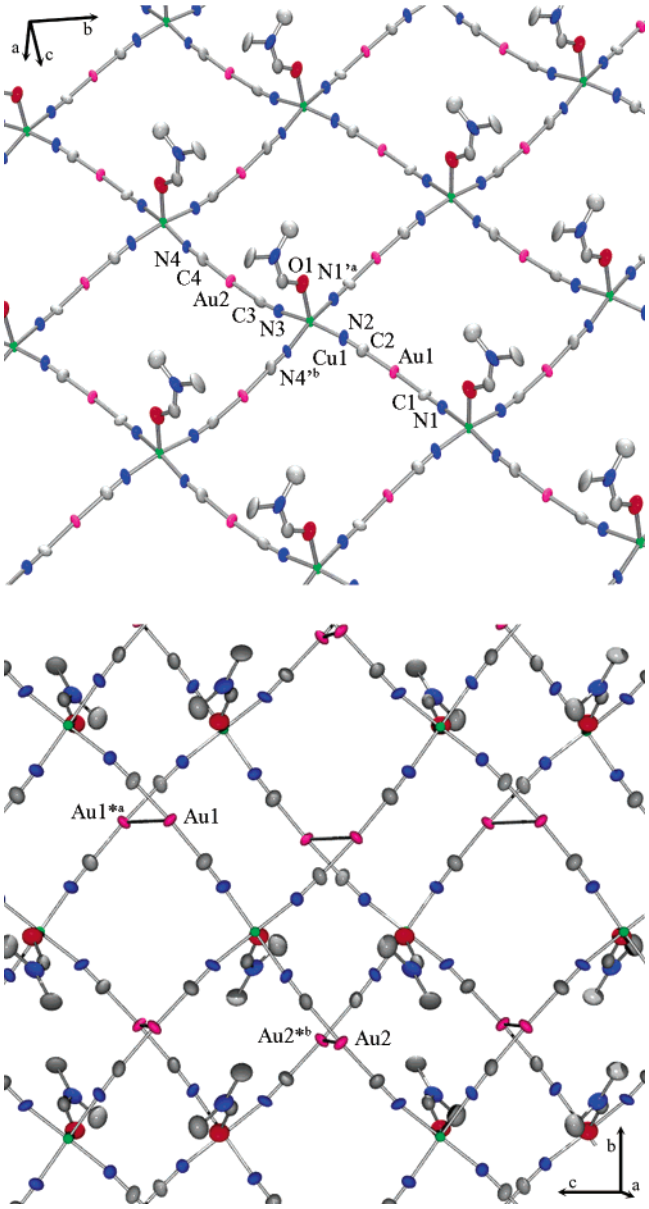

Figure 6. Top: Extended structure of **3** showing the 2-D layers (hydrogen atoms were removed for clarity). Bottom: Aurophilic interactions between the layers yield a 3-D network.

Selected bond lengths and angles for **3** are listed in Table 4. The alternation of Cu^{II} centers and $[Au(CN)_2]^-$ units generates a 2-D square grid motif with all the DMF molecules pointing either above or below the plane of the sheet (Figure 6 top). This grid is similar to that observed in the blue $Cu[Au(CN)_2]_2(DMSO)_2$ complex (**2**) if one DMSO molecule was removed and the corrugation reduced. The layers stack on top of each other in an offset fashion, thereby disrupting any channels, and are held together by Au(1)−Au(1*[a]) and Au(2)−Au(2*[b]) interactions of 3.3050(12) Å and 3.1335(13) Å (Figure 6 bottom).

Crystal Structure of $Cu[Au(CN)_2]_2(pyridine)_2$, 4. The structure of **4** is similar to that of **3**, except that the Cu^{II} centers are surrounded by two solvent molecules, generating octahedrally coordinated metals. The axial sites and two of the equatorial sites are occupied by N(cyano) atoms of bridging $[Au(CN)_2]^-$ units. Pyridine molecules occupy the two other

(41) Noro, S.-i.; Kitaura, R.; Kondo, M.; Kitagawa, S.; Ishii, T.; Matsuzaka, H.; Yamashita, M. *J. Am. Chem. Soc.* **2002**, *124*, 2568−2583.
(42) Seki, K. *Chem. Commun.* **2001**, 1496−1497.
(43) Uemura, K.; Kitagawa, S.; Kondo, M.; Fukui, K.; Kitaura, R.; Chang, H.-C.; Mizutani, T. *Chem. Eur. J.* **2002**, *8*, 3586−3600.
(44) Eddaoudi, M.; Moler, D. B.; Li, H.; Chen, B.; Reineke, T. M.; O'Keeffe, M.; Yaghi, O. M. *Acc. Chem. Res.* **2001**, *34*, 319−330.

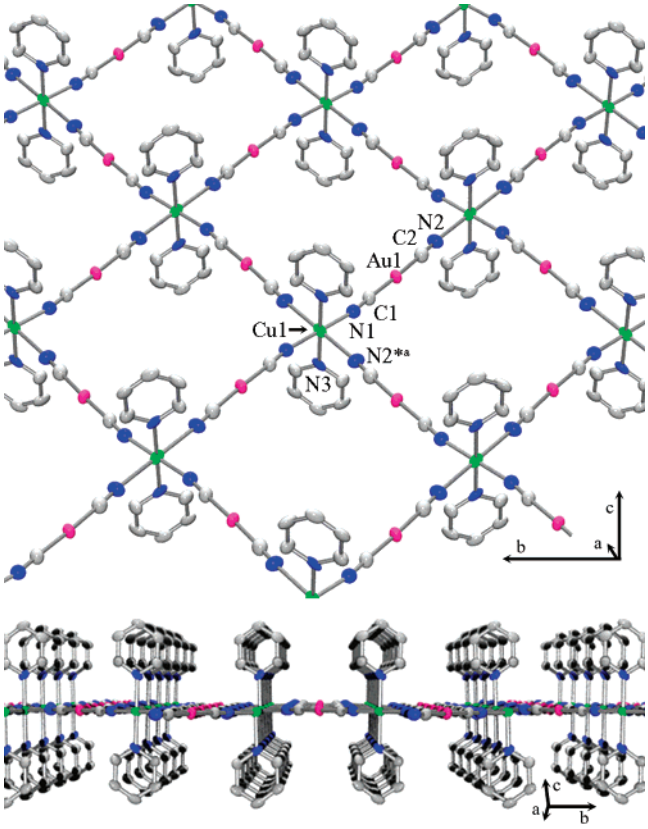

Figure 7. Top: Extended structure of **4** showing a 2-D layer. Bottom: Side view of a 2-D layer showing the pyridine ligands situated above and below the plane.

Table 5. Selected Bond Lengths (Å) and Angles (deg) for $Cu[Au(CN)_2]_2(pyridine)_2$ (**4**)[a]

Cu(1)−N(1)	2.016(9)	Cu(1)−N(3)	2.007(7)
Cu(1)−N(2*[a])	2.532(9)		
N(1)−Cu(1)−N(2*[a])	89.5(4)	C(2)−Au(1)−C(1)	177.8(4)
N(1′)−Cu(1)−N(2*[a])	90.5(4)	Cu(1)−N(1)−C(1)	169.7(9)
N(1)−Cu(1)−N(3)	90.0(3)	Cu(1*[b])−N(2)−C(2)	173.3(9)
N(1)−Cu(1)−N(3′)	90.0(3)	Au(1)−C(1)−N(1)	177.9(9)
N(2*[a])−Cu(1)−N(3)	90.4(3)	Au(1)−C(2)−N(2)	177.2(11)
N(2*[a])−Cu(1)−N(3′)	89.6(3)		

[a] Symmetry transformations: (*[a]) $x-1$, $-y+1/2$, $z-1/2$; (*[b]) $x+1$, $-y+1/2$, $z+1/2$; (′) $-x+1$, $-y$, $-z+1$.

equatorial sites. Selected bond lengths and angles for **4** are listed in Table 5. As observed for **3**, infinite 2-D layers are obtained (Figure 7). No aurophilic interactions are present between the Au atoms of neighboring sheets, but $\pi-\pi$ interactions of ~3.4 Å are found between stacked pyridine rings of adjoining sheets. Thus, the square-grid array present in **2** and **3** is maintained but in this case the sheets are completely flat, as opposed to the corrugated array found in **2**. The 180° disposition of the pyridine rings (vs the cis orientation of the DMSO molecules in **2**) also serves to separate the sheets, disrupting potential intersheet Au−Au interactions.

Solvent-Free $Cu[Au(CN)_2]_2$, 6. The green-brown solvent-free complex, $Cu[Au(CN)_2]_2$ (**6**), was also prepared by thermally removing in vacuo the water molecules from **5**. Changes in the powder X-ray diffractogram and in the ν_{CN} peaks of **6** indicate that some rearrangement in the framework occurred. The IR spectrum only shows one stretching frequency (2191 cm^{-1}), indicating that all CN groups are in a similar environment, reminiscent of the $Cu[Au(CN)_2]_2(DMF)$ structure. This is also

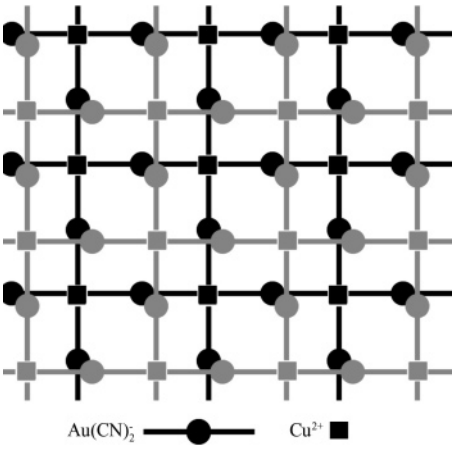

Figure 8. Postulated 2-D square grid structure of $Cu[Au(CN)_2]_2$.

comparable with the results published for the $Mn[Au(CN)_2]_2(H_2O)_2$[45] and the $Co[Au(CN)_2]_2(DMF)_2$[46] systems (which show stretches at 2150 and 2179 cm^{-1} respectively). In these two coordination polymers, the $M[Au(CN)_2]_2$ unit (M = Mn or Co) forms 2-D square grids, with solvent molecules hanging above and below the plane of the sheet. Although the three-dimensional topology of $Cu[Au(CN)_2]_2$ is not known, it likely forms a similar 2-D square grid network with all N(cyano) atoms equatorially bound to a square planar Cu^{II} center (Figure 8), as would be generated by structurally erasing the DMF molecule from **3**. The $Cu[Au(CN)_2]_2$ system was found to be only slightly porous by N_2-adsorption measurements, suggesting that the 2-D sheets stack in an offset fashion, likely with significant aurophilic interactions, thereby blocking channel formation. Despite this, solvents are still taken up by this system to yield the same $Cu[Au(CN)_2]_2(solvent)_x$ complexes.

Discussion

Results obtained by X-ray crystallography and elemental analysis indicate that **1** and **2** are true polymorphs or supramolecular isomers, as opposed to pseudopolymorphs that differ by incorporation of varying amounts or identities of cocrystallized solvent molecules.[3,4] As many factors contribute to the preferential formation of one polymorph over another, it can often be a challenge to control the synthesis of a desired isomer.[3−7] Varying crystallization conditions, such as solvent type, starting materials, temperature and concentration are key to generating just one polymorph. For example, crystallizing $Ni[Au(CN)_2]_2(en)_2$ (en = 1,2-ethylenediamine) from $[Ni(en)_3]Cl_2{\cdot}2H_2O$ or $[Ni(en)_2Cl_2]$ generates molecular and 1-D polymorphic materials, respectively.[39] Also, it has been shown that metastable polymorphs can be obtained by rapid crystallization from a supersaturated solution, e.g., via a fast drop in temperature.[6,47] For example, $\{Cu[N(CN)_2]_2(pyrazine)\}_n$ forms green/blue and blue polymorphs when crystallized from concentrated and dilute solution, respectively.[48]

Similarly, in the $Cu[Au(CN)_2]_2(DMSO)_2$ system, if the total concentration of reagents is below 0.2 M, **1** is formed, whereas

(45) Dong, W.; Zhu, L.-N.; Sun, Y.-Q.; Liang, M.; Liu, Z.-Q.; Liao, D.-Z.; Jiang, Z.-H.; Yan, S.-P.; Cheng, P. *Chem. Commun.* **2003**, 2544−2545.
(46) Colacio, E.; Lloret, F.; Kivekaes, R.; Ruiz, J.; Suarez-Varela, J.; Sundberg, M. R. *Chem. Commun.* **2002**, 592−593.
(47) Bernstein, J.; Davey, R. J.; Henck, J.-O. *Angew. Chem., Int. Ed.* **1999**, *38*, 3440.
(48) Jensen, P.; Batten, S. R.; Fallon, G. D.; Hockless, D. C. R.; Moubaraki, B.; Murray, K. S.; Robson, R. *J. Solid State Chem.* **1999**, *145*, 387−393.

Table 6. Maximum Solid-State Visible Reflectance (nm) and Cyanide ν_{CN} Absorptions (cm^{-1}) for Different $Cu[Au(CN)_2]_2(solvent)_x$ Complexes

	complex	maximum visible reflectance	ν_{CN} absorption(s) from solution	ν_{CN} absorption(s) from adsorption[a]
(**1**)	$Cu[Au(CN)_2]_2(DMSO)_2$	550 ± 7	2183(s), 2151(s)	2184(s), 2151(s) (from **5**)
(**2**)	$Cu[Au(CN)_2]_2(DMSO)_2$	535 ± 15 (broad)	2206(m), 2193(s), 2175(m), 2162(m)	
(**3**)	$Cu[Au(CN)_2]_2(DMF)$	498 ± 7	2199(s)	2199 (s)
(**4**)	$Cu[Au(CN)_2]_2(pyridine)_2$	480 ± 15 (broad)	2179(m), 2167(s), 2152(m), 2144(m)	2179(m), 2167(s), 2152(m), 2144(m)
(**5**)	$Cu[Au(CN)_2]_2(H_2O)_2$	535 ± 5	2217(s), 2194(w), 2172(s)	2217(s), 2194(w), 2171(s) (from **1**) 2216(s), 2196(w), 2171(s) (from **2**)
(**6**)	$Cu[Au(CN)_2]_2$	560 ± 20 (v. broad)	2191(s)	
(**7**)	$Cu[Au(CN)_2]_2(CH_3CN)_2$		2297(w), 2269(w), 2191(s)	
(**8**)	$Cu[Au(CN)_2]_2(dioxane)(H_2O)$	505 ± 15 (broad)	2201(s), 2172(w)	2200(s), 2174 (w)
(**9**)	$Cu[Au(CN)_2]_2(NH_3)_4$	433 ± 7		2175(m), 2148(s)

[a] All solvent adducts were made from **2** unless specified.

2 is obtained exclusively from > 0.5 M solutions. The concentration-controlled synthesis of structural isomers of coordination polymers is uncommon relative to examples with molecular systems.[48,49] This concentration dependence suggests that green **1** is the thermodynamic product, while blue **2**, which rapidly precipitates from solution, is likely a kinetic product. The fact that $Cu[Au(CN)_2]_2(H_2O)_2$ converts exclusively to the green polymorph **1** when adsorbing DMSO is further evidence that **1** is the most energetically favorable polymorph. Interestingly, the density of thermodynamically preferred **1** is actually lower than that of **2**. This surprising situation has been observed in other polymorphs.[10] Although it is unclear if this result can be attributed to entropic or enthalpic contributions, it is conceivable that the formation of shorter Au−Au bonds in **1** relative to **2** could be an important energetic factor.

It has been recognized that a system does not need to be porous in order to undergo guest uptake.[50] For example, a flexible metal−ligand superstructure can dynamically adapt in order to accommodate a variety of potential guests.[50−56] In this light, the Jahn−Teller influenced flexible coordination sphere and the greater lability of Cu^{II} compared with other transition metals are likely important features of the $Cu[Au(CN)_2]_2(solvent)_x$ system. The related $Mn[Au(CN)_2]_2(H_2O)_2$ and $Co[Au(CN)_2]_2(DMF)_2$ systems previously reported form more rigid frameworks.[45,46] For these two systems, thermal treatment is required to remove the guest molecules and yield compounds exhibiting zeolitic properties. The lability of Cu^{II} in our system facilitates the reversible exchange of adsorbed solvent molecules without any thermal treatment required. It also likely increases the flexibility of the framework by allowing the breaking and the reformation of Cu−N(cyano) bonds, thereby adapting to the solvent guest present. Gold−gold interactions appear to be present in most of the $Cu[Au(CN)_2]_2(solvent)_x$ complexes and probably help to stabilize the 3-D network as solvent exchange takes place.

Taking into account the varied structures of the $Cu[Au(CN)_2]_2(solvent)_x$ complexes, several modes of flexibility within the fundamental structural framework, i.e., the 2-D square-grid network of the $Cu[Au(CN)_2]_2$ moiety (Figure 8), can be identified. First, the 2-D square-grid can lie entirely flat, as in the mono-DMF or bis-pyridine complexes **3** and **4**, or it can buckle to generate a corrugated 2-D array, as observed in the blue bis-DMSO polymorph **2**. The extent of this corrugation can even force the partial fragmentation of the square array via the breaking of one Cu−N(cyano) bond, as observed in the green bis-DMSO polymorph **1**. Such fragmentation is probably also present in the $Cu[Au(CN)_2]_2(NH_3)_4$ complex (**9**); the Cu^{II} center in **9** is likely still octahedral, with two Cu−N(cyano) bonds (out of four in the fundamental square-grid structure) breaking completely to make way for two additional NH_3 ligands, thereby disrupting the 2-D array. Another mode of flexibility lies in the ability of the Cu^{II} center to readily alternate between being five- and six-coordinate, as well as accessing a range of five-coordinate geometries. This adaptability is independent of the extent of corrugation: five-coordinate Cu^{II} centers are found in both flat **3** and corrugated **1** while six-coordinate centers are present in both flat **4** and corrugated **2**. Finally, the Jahn−Teller distortions endemic to Cu^{II} complexes yield a third mode of flexibility: the arrangement of equatorial/axial or basal/apical N(cyano) ligands and donor solvents. Again, this pliability is independent of the extent of corrugation: both the five-coordinate DMF complex **3** and six-coordinate bis-pyridine complex **4** contain flat $Cu[Au(CN)_2]_2$ square-grids, but in **3** the N(cyano) ligands are all basal (and therefore have roughly identical Cu−N bond lengths) while in **4** two N(cyano) ligands are equatorial and two are axial, leading to significantly different Cu−N(cyano) bond lengths. This form of structural flexibility is particularly important since substantially different IR signatures in the cyanide region are generated depending on the N(cyano) bonding arrangement in the system. Of course, all three modes of flexibility work in concert to generate the adaptable, dynamic network solid that is ultimately able to bind and sense different donor solvents.

(49) Barnett, S. A.; Blake, A. J.; Champness, N. R.; Wilson, C. *Chem. Commun.* **2002**, 1640−1641.
(50) Atwood, J. L.; Barbour, L. J.; Jerga, A.; Schottel, B. L. *Science* **2002**, *298*, 1000−1002.
(51) Cote, A. P.; Shimizu, G. K. H. *Chem. Commun.* **2001**, 251−252.
(52) Edgar, M.; Mitchell, R.; Slawin, A. M.; Lightfoot, P.; Wright, P. A. *Chem. Eur. J.* **2001**, *7*, 5168−5175.
(53) Miller, P. W.; Nieuwenhuyzen, M.; Xu, X.; James, S. L. *Chem. Commun.* **2002**, 2008−2009.
(54) Lozano, E.; Nieuwenhuyzen, M.; James, S. L. *Chem. Eur. J.* **2001**, *7*, 2644−2651.
(55) Kitaura, R.; Fujimoto, K.; Noro, S.-i.; Kondo, M.; Kitagawa, S. *Angew. Chem., Int. Ed.* **2002**, *41*, 133−135.
(56) Côté, A. P.; Ferguson, M. J.; Khan, K. A.; Enright, G. D.; Kulynych, A. D.; Dalrymple, S. A.; Shimizu, G. K. H. *Inorg. Chem.* **2002**, *41*, 287−292.

The source of the vapochromism in the $Cu[Au(CN)_2]_2(solvent)_x$ system differs from that of other Au^I-containing systems.[14−17] $Cu[Au(CN)_2]_2(solvent)_x$ shows vapochromism in the visible since each donor solvent molecule that is adsorbed binds to the Cu^{II} center and modifies differently the crystal field splitting. As a consequence, the color of the vapochromic compound changes as the d−d absorption bands shift with donor. In addition to donor identity, the resulting coordination number (five or six) and specific geometry of the copper center also influences the color of the complexes by altering the splitting of the d-orbitals. Although $[Au(CN)_2]$-containing compounds are luminescent,[57−60] preliminary studies have shown that none of the $Cu[Au(CN)_2]_2(solvent)_x$ complexes are significantly luminescent, probably due to quenching by the Cu^{II} ions.

The $[Au(CN)_2]^-$ unit is also a key component of this system since it telegraphs the changes in solvent bound to the Cu^{II} centers via the ν_{CN} stretch. Each $Cu[Au(CN)_2]_2(solvent)_x$ has a different IR signature since every VOC modifies in a different manner the electron density distribution around the Cu^{II} center. This influences the amount of π-back-bonding from the Cu^{II} center to the CN group, which in turn is observed in the IR spectrum due to the change in vibration frequency.[32] Also, the number of bands observed is related to the symmetry and coordination number of the Cu^{II} centers, as described in detail above. This use of this intense, sensitive IR signature of the coordination polymer framework to report on the nature of the guest, in addition to the visible vapochromism, sets the $Cu[Au(CN)_2]_2(solvent)_x$ system apart from other vapochromic materials. Although the use of IR spectroscopy to study the sorption of VOCs by vapochromic materials has been previously reported,[21,61,62] the IR signatures in the $Cu[Au(CN)_2]_2$ system are unusually diagnostic for particular solvents/guests. For example, in systems containing $[Pt(CN)_4]^{2-}$ units, slight shifts in the ν_{CN} stretch are observed if hydrogen-bonding between the N(cyano) atoms and the VOC molecules present in the lattice occurs. VOCs cannot be differentiated or identified via IR in this case since ν_{CN} shifts of only 0−10 cm^{-1} are usually observed.[21,61,62] In the $Cu[Au(CN)_2]_2(solvent)_x$ system, changes in the number of bands (from one to four) are observed in addition to larger ν_{CN} shifts, varying between 10 and 40 cm^{-1} as solvents are exchanged.

Conclusion

It has been illustrated that, despite their different solid-state structures, the two $Cu[Au(CN)_2]_2(DMSO)_2$ polymorphs exhibit the same vapochromic behavior with respect to sorption of VOCs. The use of $[Au(CN)_2]^-$ as a building block is important to the function of this vapochromic coordination polymer. First, it provides the very sensitive CN reporter group that can allow IR-identification of the solvent adsorbed in the materials. Also, Au−Au interactions via the $[Au(CN)_2]^-$ units increase the structural dimensionality of the system in most cases and probably help provide stabilization points for the flexible $Cu[Au(CN)_2]_2$ framework.

We are currently exploring the sensitivity, selectivity, kinetics, and gas sensing capability of this coordination polymer family.

Acknowledgment. This work was supported by FQRNT of Québec (J.L.), NSERC of Canada and the World Gold Council. We are grateful to Prof. Ian Gay (Simon Fraser University) for conducting N_2-adsorption porosity measurements and to Michael Katz for helping to solve the crystal structures.

Note Added after ASAP Publication. After this paper was published ASAP on November 16, 2004, errors in the chemical formula in the article title, and in the titles of Tables 2 and 3, were corrrected. The corrected version was posted November, 17, 2004.

Supporting Information Available: X-ray crystallographic file (CIF) for $Cu[Au(CN)_2]_2(DMSO)_2$ **1** and **2**, $Cu[Au(CN)_2]_2(DMF)$ **3** and $Cu[Au(CN)_2]_2(pyridine)_2$ **4**, and TGA data for all solvent adducts. This material is available free of charge via the Internet at http://pubs.acs.org.

JA049069N

(57) Stender, M.; Olmstead, M. M.; Balch, A. L.; Rios, D.; Attar, S. *J. Chem. Soc., Dalton Trans.* **2003**, 4282−4287.
(58) Assefa, Z.; Omary, M. A.; McBurnett, B. G.; Mohamed, A. A.; Patterson, H. H.; Staples, R. J.; Fackler, J. P., Jr. *Inorg. Chem.* **2002**, *41*, 6274−6280.
(59) Assefa, Z.; Shankle, G.; Patterson, H. H.; Reynolds, R. *Inorg. Chem.* **1994**, *33*, 2187−2195.
(60) Stender, M.; White-Morris, R. L.; Olmstead, M. M.; Balch, A. L. *Inorg. Chem.* **2003**, *42*, 4504−4506.
(61) Daws, C. A.; Exstrom, C. L.; Sowa, J. R., Jr.; Mann, K. R. *Chem. Mater.* **1997**, *9*, 363−368.
(62) Exstrom, C. L.; Pomije, M. K.; Mann, K. R. *Chem. Mater.* **1998**, *10*, 942−945.